# Structural Design, Synthesis and Structure–Activity Relationships of Thiazolidinones with Enhanced Anti-*Trypanosoma cruzi* Activity

Diogo Rodrigo Magalhães Moreira,*[a, e] Ana Cristina Lima Leite,[b]
Marcos Verissimo Oliveira Cardoso,[b] Rajendra Mohan Srivastava,[a]
Marcelo Zaldini Hernandes,[b] Marcelo Montenegro Rabello,[b] Luana Faria da Cruz,[c]
Rafaela Salgado Ferreira,[c] Carlos Alberto de Simone,[d] Cássio Santana Meira,[e]
Elisalva Teixeira Guimaraes,[e, f] Aline Caroline da Silva,[g] Thiago André Ramos dos Santos,[g]
Valéria Rêgo Alves Pereira,[g] and Milena Botelho Pereira Soares[e, h]

Pharmacological treatment of Chagas disease is based on benznidazole, which displays poor efficacy when administered during the chronic phase of infection. Therefore, the development of new therapeutic options is needed. This study reports on the structural design and synthesis of a new class of anti-*Trypanosoma cruzi* thiazolidinones (**4a–p**). (2-[2-Phenoxy-1-(4-bromophenyl)ethylidene)hydrazono]-5-ethylthiazolidin-4-one (**4h**) and (2-[2-phenoxy-1-(4-phenylphenyl)ethylidene)hydrazono]-5-ethylthiazolidin-4-one (**4l**) were the most potent compounds, resulting in reduced epimastigote proliferation and were toxic for trypomastigotes at concentrations below 10 μM, while they did not display host cell toxicity up to 200 μM. Thiazolidinone **4h** was able to reduce the in vitro parasite burden and the blood parasitemia in mice with similar potency to benznidazole. More importantly, *T. cruzi* infection reduction was achieved without exhibiting mouse toxicity. Regarding the molecular mechanism of action, these thiazolidinones did not inhibit cruzain activity, which is the major trypanosomal protease. However, investigating the cellular mechanism of action, thiazolidinones altered Golgi complex and endoplasmic reticulum (ER) morphology, produced atypical cytosolic vacuoles, as well as induced necrotic parasite death. This structural design employed for the new anti-*T. cruzi* thiazolidinones (**4a–p**) led to the identification of compounds with enhanced potency and selectivity compared to first-generation thiazolidinones. These compounds did not inhibit cruzain activity, but exhibited strong antiparasitic activity by acting as parasiticidal agents and inducing a necrotic parasite cell death.

## Introduction

Chagas disease, caused by *Trypanosoma cruzi* parasite infection, affects approximately 5–10% of the Latin American population.[1,2] The standard treatment is based on benznidazole, a compound able to eliminate the parasite during the acute phase.[3] However, during the chronic phase, in which the parasite remains located inside various cell types, benznidazole is not able to eliminate the parasitism even following long-term administration.[4] Human vaccination against *T. cruzi* infection is not available,[5] and thus other therapies aiming to control infection or reduce clinical symptoms are being investigated.[6–8]

Aiming at the development of more effective medicines, a large number of anti-*T. cruzi* small molecules have been eval-

[a] Dr. D. R. M. Moreira, Prof. R. M. Srivastava
Universidade Federal de Pernambuco (UFPE)
Departamento de Química Fundamental
50670-901, Recife, PE (Brazil)
E-mail: diogollucio@gmail.com

[b] Prof. A. C. Lima Leite, Dr. M. V. O. Cardoso, Prof. M. Z. Hernandes,
M. M. Rabello
UFPE, Departamento de Ciências Farmacêuticas
50740-520, Recife, PE (Brazil)

[c] L. F. da Cruz, Prof. R. S. Ferreira
Universidade Federal de Minas Gerais (UFMG)
Departamento de Bioquímica e Imunologia
31270-901, Belo Horizonte, MG (Brazil)

[d] Prof. C. A. de Simone
Universidade de São Paolo (USP)
Departamento de Física e Informática, Instituto de Física
CEP 13560-970, São Carlos, SP (Brazil)

[e] Dr. D. R. M. Moreira, C. S. Meira, Dr. E. T. Guimaraes, Dr. M. B. Pereira Soares
Fundação Oswaldo Cruz (Fiocruz), Centro de Pesquisas Gonçalo Moniz
CEP 40296-710, Salvador, BA (Brazil)

[f] Dr. E. T. Guimaraes
Universidade do Estado da Bahia (UNEB)
Departamento de Ciências da Vida
41150-000, Salvador, BA (Brazil)

[g] A. C. da Silva, T. A. R. dos Santos, Dr. V. R. A. Pereira
FIOCRUZ, Centro de Pesquisas Aggeu Magalhaes
50670-420, Recife, PE (Brazil)

[h] Dr. M. B. Pereira Soares
Centro de Biotecnologia e Terapia Celular, Hospital São Rafael
41253-190, Salvador, BA (Brazil)

Supporting information for this article is available on the WWW under
http://dx.doi.org/10.1002/cmdc.201300354.

uated. To date, compounds that in some way inhibit either the trypanosomal protease cruzain or the ergosterol biosynthesis are the most outstanding *T. cruzi* growth inhibitors.[9–12] In fact, some of these compounds have exhibited strong activity in reducing parasitemia in *T. cruzi*-infected mice as well as low toxicity in these animal models.[13–16] Given this promising outlook, the structural design of new molecules based on these *T. cruzi* molecular targets is an attractive line of research.

Hydrazones are well-known antiparasitic compounds.[17,18] Based on this, our research group has been investigating cruzain-inhibiting hydrazones to obtain novel and potent anti-*T. cruzi* agents. At least five distinct classes were investigated: thiosemicarbazones,[19] *N*-acylhydrazones,[20,21] thiazolidinones[22–24] and their transition metal complexes.[25] Within the thiazolidinone class of compounds, we identified compound **18** after examining the importance of modifications at every atom of the thiazolidinic ring (Figure 1). Compound **18** displayed an IC$_{50}$ value of $10.1 \pm 0.09$ µM to reduce the percentage of infected host cells, which is similar to the observed value for benznidazole. However, thiazolidinone **18** was less efficient in reducing blood parasitemia in *T. cruzi*-infected mice than benznidazole.[24] To identify new anti-*T. cruzi* thiazolidinones with enhanced in vivo efficacy, we reasoned that some molecular modifications in this class of compounds are necessary.

Previously, it was observed that thiazolidinone **18** inhibits cruzain activity but not its homologous in mammalian cells (cathepsin L).[24] However, it was several times less potent than KB2, a high-efficient cruzain inhibitor.[13] A comparison of cruzain docking between **18** and KB2 has revealed that the major difference is that KB2 assumes a T-shaped conformation. Therefore, we hypothesized that thiazolidinones displaying a conformation resembling the KB2 might enhance activity against cruzain, and consequently, against parasite cells. To achieve this, it was necessary to disrupt the existent planarity between the phenoxyl group and the thiazolidinic ring. Based on literature findings,[26,27] the attachment of an aryl ring to the iminic carbon should produce thiazolidinones with greater conformational restriction (i.e., high rotational energy barrier) than observed in **18**, and, consequently, produce thiazolidinones with the desirable T-shaped conformation (Figure 2).

Based on this structural design, new thiazolidinones denoted as compounds **4a–p** were synthesized and evaluated as antiparasitic agents as well as cruzain inhibitors. Initially, compound **4a** was prepared, which contains a phenyl ring attached to the iminic carbon. To determine the importance of this phenyl for the activity, compounds containing a pyridinyl instead of a phenyl ring were synthesized. Thereafter, substituents attached to the phenyl ring were examined, such as, alkyl,
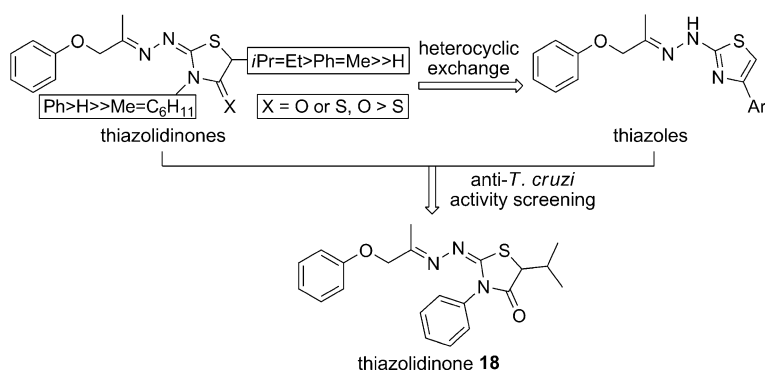


**Figure 1.** SARs of the previously studied anti-*T. cruzi* agents. Thiazolidinone **18** was identified as the most potent compound among them.
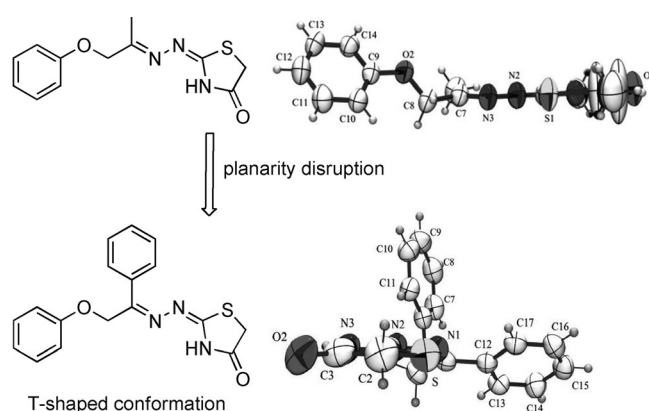


**Figure 2.** Thiazolidinones previously investigated (top) and proposed here (bottom). Crystal structures (Ortep-3) highlight the difference of molecular planarity between the two series.

alkoxy, halogen atoms and six-membered rings. In addition, compounds containing two or three substituents attached to the phenyl ring were prepared. By evaluating the antiparasitic activity of compounds **4a–p**, we identified that thiazolidinones had stronger anti-*T. cruzi* activity compared with the previously reported thiazolidinone **18**. More importantly, we found that compounds **4h** and **4l** are as potent as benznidazole in the inhibition of *T. cruzi* infection in host cells. As expected, based on its high in vitro antiparasitic activity, mice treated orally with thiazolidinone **4h** had substantially reduced blood parasitemia, similar to the observations made with benznidazole-treated mice.

## Results

### Synthesis

The route used for synthesizing thiazolidinones **4a–p** is shown in Scheme 1. The synthesis was initiated with the reaction between commercially available ketones and bromines, which yielded α-bromoketones **1a–p**.[28] These were reacted with phenol in basic conditions to give the respective β-ketoethers **2a–p**. To prepare biphenyl compound **2l**, a Suzuki cross-cou-
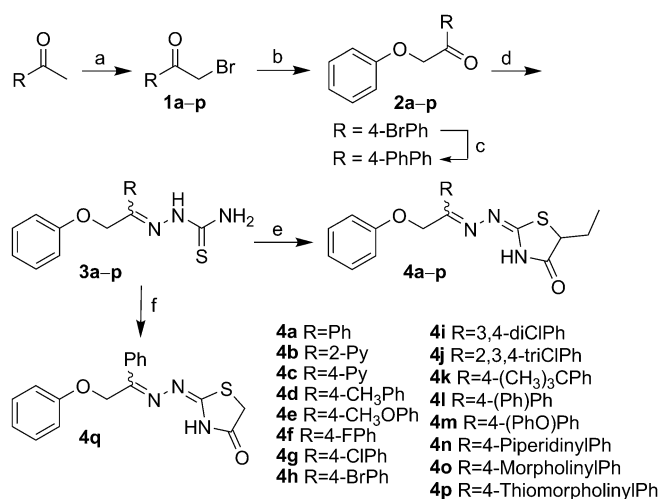
**Scheme 1.** Synthesis of thiazolidinones **4a–q**. *Reagents and conditions*: a) Br$_2$, Et$_2$O/dioxane (1:1), −5 °C, 5 h. b) Phenol, K$_2$CO$_3$, butanone, reflux, 5–10 h, 42–72%. c) Phenylboronic acid, Pd(OAc)$_2$, P(Ph)$_3$, MeOH, dioxane, 90 °C, 20 h, 50%. d) Thiosemicarbazide, EtOH, AcOH, reflux, 2 h, 43–83%. e) Ethyl 2-bromobutyrate, KOAc, EtOH, reflux, 6–8 h, 40–81%. f) Ethyl 2-bromoacetate, KOAc, EtOH, reflux, 6 h, 75%. Ph = phenyl, Py = pyridinyl.

pling reaction was performed between the bromophenyl **2h** and phenylboronic acid by using Pd(OAc)$_2$ and P(Ph)$_3$ as catalysts.[29] Reactions of β-ketoethers **2a–p** with thiosemicarbazide under acidic conditions at reflux provided thiosemicarbazones **3a–p** with yields varying from 43 to 83% and acceptable purities (approx. 95%) by simple precipitation following recrystallization. Cyclizations of thiosemicarbazones **3a–p** to thiazolidinones **4a–p** were carried out with ethyl-2-bromobutyrate in the presence of potassium acetate at reflux for six to eight hours, and thiazolidinones **4a–p** were isolated as colorless solids with purities > 98% determined by elemental analysis. The compounds were chemically characterized by $^1$H and $^{13}$C NMR, IR and HRMS (ESI). The $^1$H NMR spectra showed that thiazolidinones **4a–p** are composed of two diastereomers, and through analysis of the HPLC chromatograms, we determined that the ratio of the isomer mixture **4a/4h** is 90:10.

Next, we aimed to define the configuration of the major isomer by crystallographic analysis. We did not succeed in crystallizing thiazolidinones **4a–p** suitable for X-ray analysis. Because previously we observed that thiazolidinic derivatives without substituents attached to the heterocyclic ring are more prone to afford crystals suitable for X-ray measurements, we decided to prepare thiazolidinone **4q** for X-ray analysis. After recrystallization and chromatographic purification of **4q**, its major isomer was isolated, and a single crystal suitable for X-ray analysis was collected. As shown in the Ortep-3 representation of thiazolidinone **4q**, carbon C5 and nitrogen N2 are on the same side, characteristic of a *Z* configuration in regard to the C4=N1 bond (Figure 3). Interestingly, the phenyl ring attached to the iminic carbon is coplanar to the thiazolidinic ring, while the phenoxy ring is oriented to a different side. Another interesting observation is that the double bond of C1 is located in an exocyclic position in relation to the heterocyclic ring, which gives rise to an isomerism in the C1=N2 bond.[30–32]
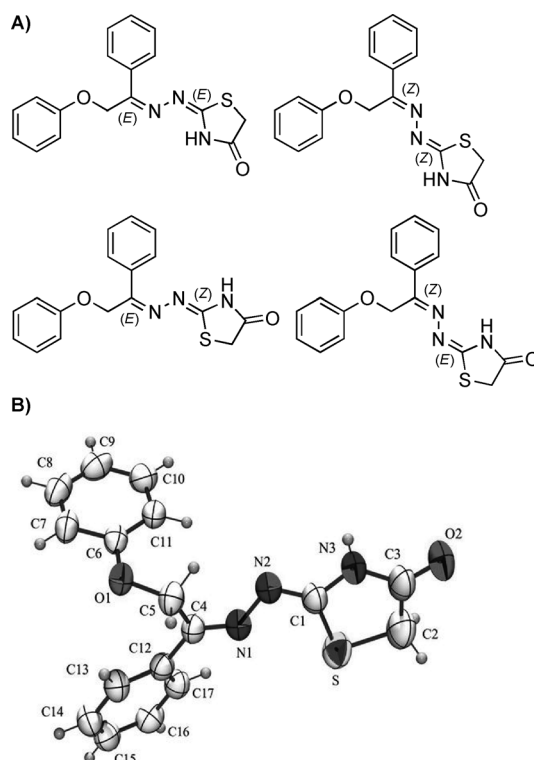


**Figure 3.** A) Structures of the possible diastereoisomers and B) Ortep-3 representation for the crystal structure of thiazolidinone **4q**.
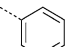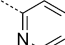
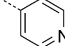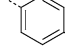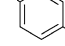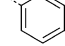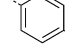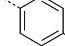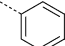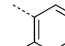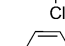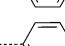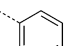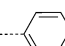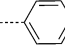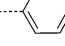In the crystalline structure depicted in Figure 3, N2 and the sulfur atom are on the same side, characterizing a *Z* configuration for the C1=N2 bond. Thiazolidinone **4q** showed $^1$H NMR chemical shifts similar to thiazolidinones **4a–p**; therefore, it is fair to suggest that the major isomer for thiazolidinones **4a–p** has a *Z* configuration in regard to the C4=N1 bond. Important to note is that all compounds were used in the pharmacological tests as isomer mixtures.

## Antiparasitic activity against extracellular forms and cytotoxicity against host cells

First, compounds **4a–p** were evaluated against epimastigotes and trypomastigotes of *T. cruzi*. Antiparasitic activity was determined by counting the parasite number in a Neubauer chamber and calculating the concentration of the test compound resulting in 50% inhibition (IC$_{50}$, epimastigotes) or 50% cytotoxicity (CC$_{50}$, trypomastigotes). Cytotoxicity in host cells was determined in mouse splenocytes, measured by the incorporation of [$^3$H]-thymidine, and results were expressed as the highest non-cytotoxic concentration (HNC). Benznidazole was used as reference antiparasitic drug and exhibited a CC$_{50}$ value of 6.0 μM against trypomastigotes. As cut-off, compounds with CC$_{50}$ values ≤ 6.0 μM against trypomastigotes were considered potent anti-*T. cruzi* compounds. The results are reported in Table 1.

We first analyzed the antiparasitic activity against trypomastigotes. The nonsubstituted phenyl derivative **4a** was active but was less potent than benznidazole. The replacement of

**Table 1.** Anti-*T. cruzi* activity, cytotoxicity and cruzain inhibition.

| Compd | R | *T. cruzi* CC$_{50}$ [µM][a] trypomastigotes | *T. cruzi* IC$_{50}$ [µM][b] epimastigotes | Splenocytes HNC [µM][c] | Cruzain Inhibition [%][d] |
|---|---|---|---|---|---|
| 4a | | 17.7 | 25.0 | >283 | 64±2 |
| 4b | | >100 | >100 | 28 | 5±5 |
| 4c | | >100 | 67.8 | 28 | 11±2 |
| 4d | | 97.2 | ND | >272 | 36.1±0.6 |
| 4e | | 82.0 | ND | >261 | 58±5 |
| 4f | | 78.9 | >100 | >269 | 37±2 |
| 4g | | 17.3 | 11.3 | 258 | 50.4±0.3 |
| 4h | | 4.0 | 3.9 | >231.4 | 40±13 |
| 4i | | 50.8 | ND | 237 | 25±2 |
| 4j | | ND | >100 | 21.9 | 13±3 |
| 4k | | 74.9 | >100 | >244 | 0 |
| 4l | | 10.8 | 11.1 | >233 | 18±2 |
| 4m | | 68.5 | >100 | >244 | 31±2 |
| 4n | | 12.7 | 1.8 | 57.3 | 78±2 (0.7±0.4) |
| 4o | | 15.9 | >100 | 22.8 | 15±2 |
| 4p | | 10.8 | 31.9 | 22.0 | 94.3±0.9 (4.0±0.5) |
| Bdz | | 6.0 | 4.8 | 96.1 | – |
| Sap | | – | – | 1.0 µg mL$^{-1}$ | – |

[a] Determined 24 h after incubation of Y strain trypomastigotes with the test compounds. [b] Determined 5 days after incubation of Dm28c-strain epimastigotes with the test compounds. [a,b] Only values with a standard deviation <10% were included. [c] Highest noncytotoxic (HNC) concentration for mouse splenocytes after 24 h of incubation in the presence of the test compounds. [d] Compounds were tested at 100 µM and the percent inhibition of catalytic activity was determined; values in parenthesis are IC$_{50}$ values [nM] and represent the mean±SD of three measurements. ND=not determined due to lack of activity; NT=not tested; Bdz=benznidazole; Sap=saponin.

resulted in a fourfold increase in activity and produced a derivative that was as potent as benznidazole. In contrast, attaching two (**4i**) or three chloro (**4j**) substituents decreased anti-*T. cruzi* activity.

Compound **4l**, carrying a biphenyl group, displayed an activity similar to benznidazole-treated parasites. In practice, the 4-bromophenyl derivative **4h** and biphenyl derivative **4l** are equipotent antitrypanosomal agents. The 4-phenoxy derivative **4m** exhibited a CC$_{50}$ value of 68.5 µM, being inactive in practice. In comparison to the nonsubstituted phenyl derivative **4a**, the piperidinyl derivative **4n** was slightly more active. The same was observed when a morpholinyl (**4o**) or a thiomorpholinyl (**4p**) substituent was attached. Overall, **4h** was identified as the most potent cidal agent against trypomastigote, while six other compounds (**4a**, **4g**, **4l**, and **4n**–**p**) also showed considerable antiparasitic activity (CC$_{50}$ < 10 µM), but they were less potent than benznidazole.

Next, we analyzed the antiparasitic activity against epimastigotes. Benznidazole, which was used as the reference drug, exhibited an IC$_{50}$ value of 4.8 µM. In comparison, the nonsubstituted phenyl derivative **4a** was several times less potent (IC$_{50}$ = 25 µM). The 4-bromo derivative **4h** was very active in inhibiting epimastigote and displayed an IC$_{50}$ value of 3.9 µM. In fact, this compound was as potent as benznidazole. In contrast, the biphenyl derivative **4l** was active in inhibiting epimastigotes (IC$_{50}$ = 11.1 µM) but was only half as potent as benznidazole.

After determining the antiparasitic activity, we evaluated the cytotoxicity in host cells. Saponin was used as the reference drug in this assay, while benznidazole was evaluated to compare the cytotoxicity. As shown in Table 1, compounds **4a**–**p** were less cytotoxic than saponin. In comparison to benznidazole, only five derivatives **4b**, **4c**, **4n**, **4o**, and **4p** were equally or more cytotoxic, whereas the rest of the derivatives were less cytotoxic. Derivatives **4h** and **4l**, which are the most potent

the phenyl ring (**4a**) by 2- and 4-pyridinyl (**4b** and **4c**, respectively) produced inactive thiazolidinones. The attachment of a methyl (**4d**), methoxy (**4e**) and *tert*-butyl (**4k**) substituent at the 4-position of the phenyl ring decreased the antiparasitic activity. The attachment of 4-fluoro (**4f**) also decreased the activity; however, attaching a 4-chloro (**4g**) produced a compound as active as the nonsubstituted phenyl derivative (**4a**). A further increase in potency was achieved by replacing the nonsubstituted phenyl ring (**4a**) with a 4-bromo (**4h**), which
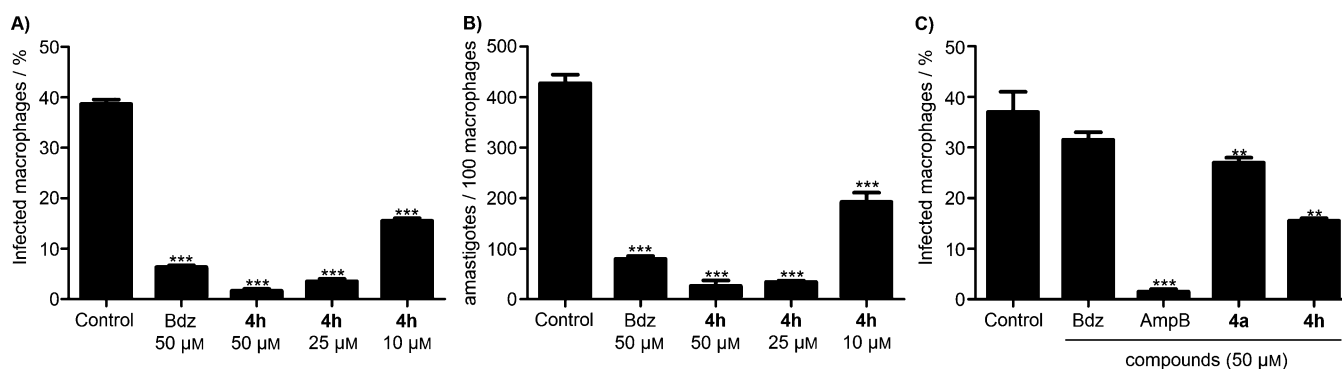
**Figure 4.** Thiazolidinone **4h** reduces the parasite development and invasion process in host cells. A,B) *T. cruzi*-infected macrophages were treated and incubated for 4 days. A) Infected cells in percent. B) Mean number of intracellular amastigotes per 100 infected macrophages. C) Macrophages were simultaneously exposed to trypomastigotes and treatment. The cell culture was incubated for 2 h, washed and the percent of infected cells was determined after 2 h. Bdz = benznidazole, AmpB = amphotericin B. Data are the mean ± S.E.M. (error bars) of two independent experiments performed. Panels A and B: ***, $p < 0.001$; panel C: ***, $p < 0.001$; **, $p < 0.01$.

anti-*T. cruzi* compounds among the series, did not exhibit cytotoxicity for splenocytes at concentrations up to 200 μM.

### In vitro infection and selectivity index

After evaluating the antiparasitic activity against the extracellular parasite, we analyzed the activity against the intracellular parasite. In this assay, *T. cruzi*-infected macrophages were treated and incubated for 96 h. Benznidazole was used as a reference drug, and the results are summarized in Figure 4 A,B. In comparison to untreated cells, treatment with **4h** reduced the percentage of infected cells ($p < 0.001$) as well as the mean number of intracellular amastigotes per 100 macrophages. Next, we investigated whether **4h** inhibits the *T. cruzi* invasion process in macrophages. To study this, macrophages were infected with trypomastigotes and simultaneously treated. After 2 h, unbound parasites were removed, and the cells were incubated for 2 h. Benznidazole and amphotericin B were used as reference drugs (Figure 4 C). In comparison to untreated cells, treatment with **4h** or **4l** reduced the percentage of infected macrophages ($p < 0.01$); however, this reduction was smaller than observed under amphotericin B treatment ($p < 0.001$). In this parasite invasion assay, benznidazole did not show significant activity.

Because the activity of **4h** was concentration-dependent, we determined its IC$_{50}$ value and selectivity index (SI) in the in vitro infection assay (see Table 2). Compound **4h** was twice as potent as benznidazole in reducing the percentage of infected cells. In contrast, **4l** was less potent, exhibiting the same potency as benznidazole. Compound **4h** has an SI value of 44, which is two times higher than the value for **4l** as well as benznidazole.

### Cruzain inhibition and docking analysis

To investigate the mechanism of action, compounds were tested against cruzain. The inhibition of cruzain enzymatic activity by all compounds was measured using a competition-based assay with the substrate Z-Phe-Arg-aminomethylcou-

**Table 2.** In vitro infection, cytotoxicity in macrophages and selectivity index (SI).

| Compd | IC$_{50}$ [μM][a] | CC$_{50}$ [μM][b] | SI[c] |
|---|---|---|---|
| **4h** | 5.2 ± 0.54 | 230.5 ± 5 | 44 |
| **4l** | 10.1 ± 0.09 | 233.3 ± 9 | 23 |
| Bdz | 13.9 ± 0.39 | 250 ± 9 | 18 |

[a] IC$_{50}$ determined in *T. cruzi*-infected macrophages after incubation for 4 days. [b] CC$_{50}$ determined in mouse splenocytes after incubation for 24 h. Data represent the mean ± SD of two independent experiments performed in duplicate. [c] Determined as CC$_{50}$/IC$_{50}$. Bdz = benznidazole.

marin (Z-FR-AMC).[33] Initially, compounds were screened at 100 μM, and only compounds with an inhibition value > 70 % were chosen for IC$_{50}$ value determination (see Table 1). We observed that cruzain activity was not substantially inhibited by the presence of most thiazolidinones, except for derivatives **4n** and **4p**, which showed IC$_{50}$ values of 0.7 ± 0.4 nM and 4.0 ± 0.5 nM, respectively.

To define the structural determinants for cruzain inhibition observed for compounds **4n** and **4p**, molecular docking was performed. The binding mode for these ligands was determined by the highest (most positive) score among the possible solutions for each ligand. These calculations were generated according to the Goldscore fitness function. In order to identify the molecular reasons for the two extreme affinities towards the cruzain target, we selected the two most potent compound, (*R*)-**4n** and (*R*)-**4p**, in addition to the weak cruzain inhibitor (*S*)-**4b**. We performed a detailed analysis of the intermolecular interactions observed in the docking solutions, for these molecules. Although the two most potent molecules are very similar to each other, they differ by the replacement of a carbon atom on (*R*)-**4n** for a sulfur atom on (*R*)-**4p**. The difference between the active (*R*)-**4n** and the inactive cruzain inhibitor (*S*)-**4b** is the presence of a 2-pyridinyl instead of a 4-(piperidinyl)phenyl ring, in addition to the inversion of the chiral center. The comparative results can be found in Figure 5.

The difference between the binding modes of (*R*)-**4n** and (*S*)-**4b** is show in Figure 6 and Table 3. The residues of cruzain,
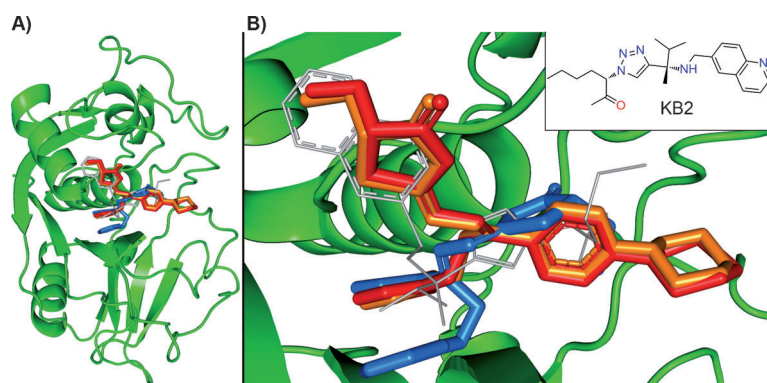
**Figure 5.** Superimposition of the docking solutions on cruzain for compounds (*R*)-**4n** (orange stick), (*R*)-**4p** (red stick), (*S*)-**4b** (blue stick) and the crystal structure of "KB2" co-crystallized ligand (gray line). A) Full and B) active site view. Inset: chemical structure of KB2.[13]
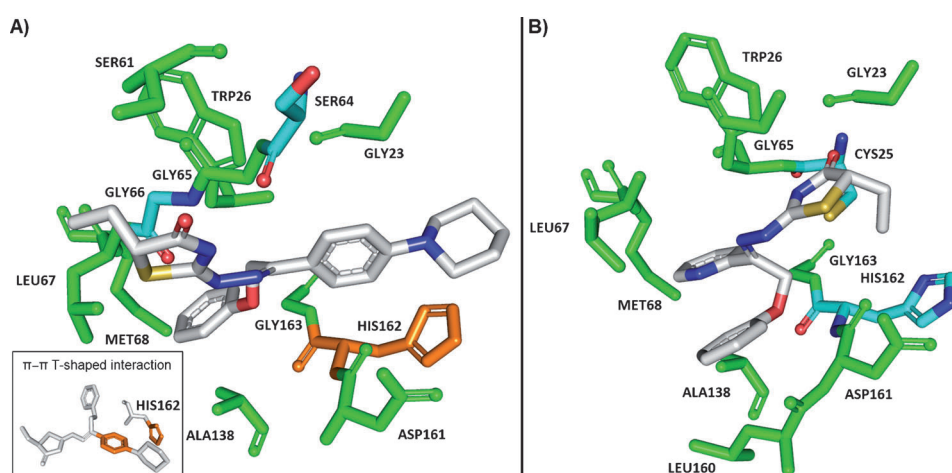


**Figure 6.** Detailed view of the docking solutions on cruzain, for A) (*R*)-**4n** and B) (*S*)-**4b**. Residues involved in hydrophobic interactions (green), hydrogen bonds (cyan), and π–π T-shaped interactions (orange) are highlighted. A detailed view of the π–π T-shaped interaction (orange) of the HIS162 residue with (*R*)-**4n** is shown in the box.

docking scores, demonstrating that the molecules with more stable or positive docking scores (in silico affinity) are the most potent cruzain inhibitors.

### Electron microscopy of parasite morphology

We analyzed the *T. cruzi* cellular membranes and organelles following thiazolidinone treatment. In this assay, trypomastigotes were treated with **4h** (4.0 μM; $CC_{50}$ value), incubated for 24 h and then cells were analyzed by transmission electron microscopy (TEM). In comparison to untreated parasites, the treatment induced the formation of an atypical dilatation of the Golgi complex and endoplasmatic reticulum (ER), as well as some distentions of the ER perinuclear membrane (Figure 7). In addition, treatment produced the formation of numerous and atypical vacuoles within the cytoplasm and in close proximity to the Golgi complex, which is commonly observed within parasite autophagy. In comparison to untreated parasites, no alterations were observed in the kinetoplast and cell nucleus in the treated parasites.

which participate in hydrophobic interactions, are highlighted in green, whereas those that participate in hydrogen bonds are highlighted in cyan. Finally, the residues involved in π–π T-shaped interactions are highlighted in orange. As shown in Figure 5, the cruzain binding mode for (*R*)-**4n** and (*R*)-**4p** is very similar. Table 3 provides a list of the molecular interactions and shows that the two compounds have many interactions in common. This similarity is also revealed when we analyze the docking score values for (*R*)-**4n** and (*R*)-**4p**, which are 55.39 and 56.48, respectively. In contrast, through comparison with the values for (*R*)-**4n** and (*R*)-**4p**, the lower affinity of (*S*)-**4b** for cruzain can also be identified. The data presented in Table 3 demonstrates that the π–π T-shaped interaction seems to be mainly responsible for the greater stability and the positioning of the complex formed between (*R*)-**4n** or (*R*)-**4p** and cruzain. The docking score calculated for (*S*)-**4b** is lower (49.59) than those calculated for the potent compounds (*R*)-**4n** or (*R*)-**4p**. Therefore, this result indicates that the most potent cruzain inhibitors (*R*)-**4n** and (*R*)-**4p** are also those with the highest

| Table 3. Molecular interaction of cruzain with (*R*)-**4n**, (*R*)-**4p** and (*S*)-**4b**. | | | |
|---|---|---|---|
| Residues | Compounds[a] | | |
| | (*R*)-**4n** | (*R*)-**4p** | (*S*)-**4b** |
| Gly 23 | HC | HC | HC |
| Cys 25 | – | – | 2.4[b] |
| Trp 26 | HC | HC | HC |
| Ser 61 | HC | HC | – |
| Ser 64 | 3.1[b] | 2.9[b] | – |
| Gly 65 | HC | HC | HC |
| Gly 66 | 3.1[b] | 3.0[b] | – |
| Leu 67 | HC | HC | HC |
| Met 68 | HC | HC | HC |
| Ala 138 | HC | HC | HC |
| Leu 160 | – | – | HC |
| Asp 161 | HC | HC | HC |
| His 162 | PIT | PIT | 2.6[b] |
| Gly 163 | HC | HC | HC |
| Scores | 55.39 | 56.48 | 49.59 |

[a] HC = hydrophobic contacts, PIT = π–π T-shaped interaction. [b] Hydrogen bond distances [Å] between donor and acceptor.
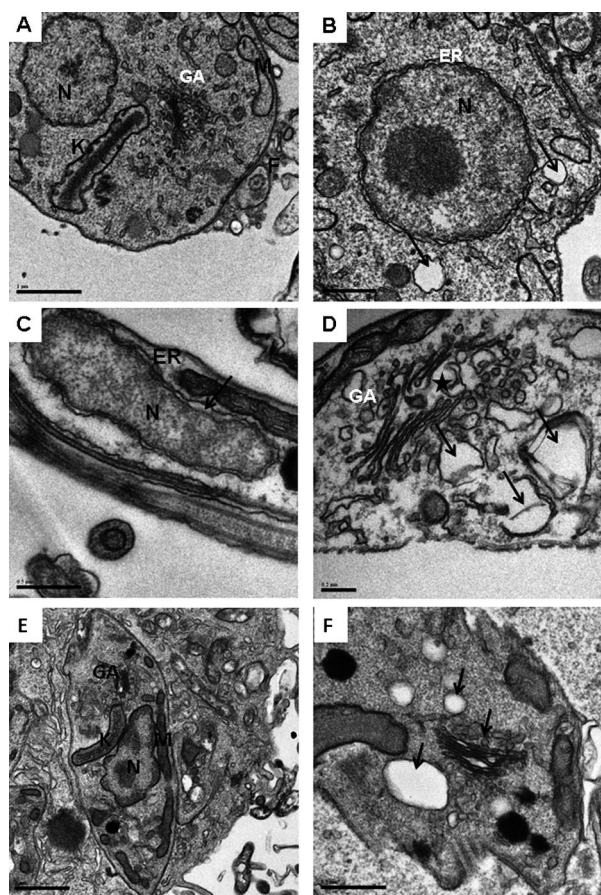
**Figure 7.** Electron microscopy analysis of parasite morphology. A) Untreated trypomastigotes analyzed by TEM. B–D) Trypomastigotes incubated for 24 h with **4 h** (4.0 μm). The formation of atypical vacuoles in the cytoplasm is shown (B). Arrows highlight alterations in the ER membrane (C). Alterations in the Golgi complex is indicated by stars (D). Untreated infected macrophages are observed after 6 h of infection (E). F) Infected macrophages incubated for 6 h with **4 h** (5.0 μm). Alterations in the Golgi apparatus and the formation of atypical vacuoles are visible (indicated by arrows). N = nucleus; K = kinetoplast; GA = Golgi apparatus; ER = endoplasmatic reticulum. Scale bars: A) 1 μm; B, C) 0.5 μm; D) 0.2 μm; E) 1 μm; F) 0.5 μm.

Next, infected macrophages were analyzed by TEM. In comparison to untreated infected macrophages, thiazolidinone treatment led to the formation of atypical cytosolic vacuoles as well as alterations in the Golgi complex morphology. These results indicate that **4 h** is a parasiticidal agent.[34]

**Parasite death process**

After ascertaining that **4 h** is a parasiticidal agent, the process of parasite death induction was studied more closely. Trypomastigotes were treated with different concentrations of **4 h** during 24, 48 and 72 h incubation and then labeled with annexin V and propidium iodide (PI). Experiments were analyzed by flow cytometry (Figure 8). In untreated parasites, most cells were negative for annexin V and PI staining, demonstrating cell viability. In comparison to untreated parasites, a significant and concentration-dependent increase in the number of PI-positive parasites was observed under treatment with **4 h**. Treatment

with 12 μm of **4 h** for 48 h resulted in 9.56 and 16.2 % of parasites positively stained for PI and PI + annexin V, respectively; whereas 1.94 % parasite cells were stained only for annexin V. These results indicate that thiazolidinone treatment increases the number of PI staining, which is characteristic of a parasite cell death caused by a necrotic process.

**Toxicology in mice**

A single-dose toxicological study was carried out for thiazolidinone **4 h**. The compound was given orally by gavage in uninfected female BALB/c mice ($n = 3$/group) at the doses of 150, 300 or 600 mg kg$^{-1}$. Mice were monitored during 14 days. To the tested doses, neither mortality nor gross signs associated to toxicity were observed (data not shown). Doses higher 600 mg kg$^{-1}$ could not be tested due to the limited solubility of **4 h** in 20 % DMSO/saline, so the maximum tolerated dose in BALB/c mice was not calculated.

In another experiment, 600 mg kg$^{-1}$ of **4 h** was administrated to a group of uninfected mice ($n = 6$) and blood samples were collected 24 h after treatment. Fourteen biochemical components of the sera were measured and the levels were compared to the negative control group (receiving vehicle; data are summarized in table S1 of the Supporting Information). In comparison to the negative control, treatment with **4 h** altered three biochemical components of the sera ($p < 0.05$): alanine aminotransferase, amylase and creatine. Alanine aminotransferase and amylase are biochemical components involved in liver function, suggesting that in this dose, compound **4 h** is potentially hepatotoxic. However, between untreated and treated groups, no statistical differences were observed for other analyzed components.

**Infection in mice**

Given the potent in vitro antiparasitic activity as well as low toxicity in mice, we tested thiazolidinone **4 h** in *T. cruzi*-infected mice (acute model). In this assay, Y strain trypomastigotes were inoculated in female BALB/c mice ($n = 6$/group). Five days after infection, mice were treated orally by gavage once a day for five consecutive days. Compound **4 h** was administrated at a dose of 125 μmol kg$^{-1}$ (55 mg kg$^{-1}$) and 250 μmol kg$^{-1}$ (110 mg kg$^{-1}$). The positive and negative control groups received benznidazole (250 μmol kg$^{-1}$, 65 mg kg$^{-1}$) and 20 % DMSO/saline, respectively. Blood parasitemia was analyzed, and the results are shown in Figure 9.

In the negative control group, blood parasitemia was observed after day 6 of parasite inoculation and peaked on day 10. In the positive control group, which received benznidazole, very low blood parasitemia was observed during the experiment, indicating that infection erradication was achieved. In comparison to the negative control group, treatment with **4 h** significantly reduced blood parasitemia in all tested doses ($p < 0.001$). All infected and treated mice survived and did not show any behavioral alterations until the end of the experiment (data not shown).
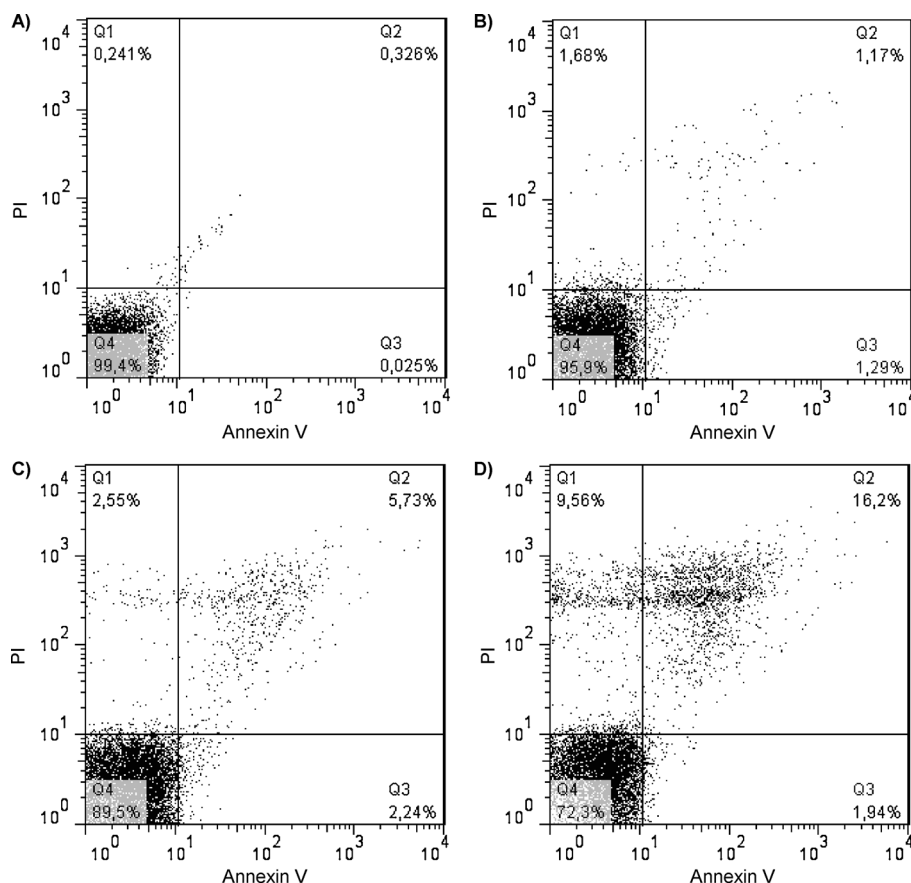
**Figure 8.** Thiazolidinones cause *T. cruzi* death by a necrotic process. Flow cytometry examination of trypomastigotes treated with **4h** within 48 h incubation. A) Untreated trypomastigotes; B) 4.0 μM; C) 8.0 μM; D) 12 μM. Two independent experiments were performed. Data are representative of one experiment.

a dose of 250 μmol kg$^{-1}$, 97% of blood parasitemia was reduced ($p < 0.001$).

### Drug combination

In another set of experiments, the antiparasitic activity of thiazolidinone **4h** alone and in combination with benznidazole was investigated in the in vitro infection assay. For this assay, compound concentrations were selected based on the IC$_{50}$ values. As shown in Table 5, neither thiazolidinone **4h** nor benznidazole alone were unable to cure the infection in macrophage culture. In contrast, the combination of **4h** plus benznidazole reduced the number of infected macrophages to greater extent than each compound used alone. The combination of the two compounds each at a concentration of 40 μM cured the infection in macrophages. More importantly, this was achieved without affecting host cell viability (data not shown).
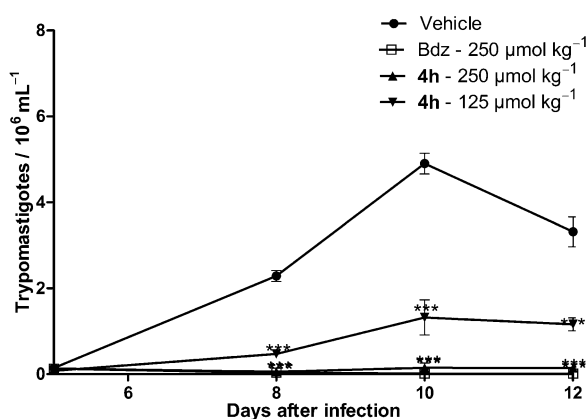


**Figure 9.** Course of acute infection and response to treatment in *T. cruzi*-infected mice. Female BALB/c mice ($n = 6$/group) were infected with trypomastigotes and treated for five consecutive days with thiazolidinone **4h** by oral gavage once a day. Blood parasitemia was monitored by counting the number of trypomastigotes. One single experiment. Error bars for S.E.M.; significance: ***, $p < 0.001$ compared to untreated (vehicle) group.

The peak parasitemia was employed to calculate the percentage of parasitemia reduction (Table 4). In comparison to the negative control, treatment with **4h** at a dose of 125 μmol/kg reduced blood parasitemia by 75.4% ($p < 0.001$). At

**Table 4.** Summary of the in vivo antiparasitic activity.

| Compd | Dose [μmol kg$^{-1}$] | Blood parasitemia reduction in mice [%][a] | |
|---|---|---|---|
| | | 8 dpi | 10 dpi |
| **4h** | 125 | 79.4 | 75.4 |
| **4h** | 250 | 97.7 | 97 |
| Bdz | 250 | 98.6 | >99 |

[a] Data taken from Figure 9, and values were calculated using the equation (vehicle group−treated group)/vehicle group]×100%. Dpi = days post-infection; Bdz = benznidazole.

**Table 5.** Summary of the in vitro antiparasitic activity of the drug combination.

| 4h [μM] | Bdz [μM] | Cell infection inhibition [%][a] |
|---|---|---|
| none | 14 | 49.7 |
| 5.5 | none | 45.2 |
| 5.5 | 14 | 81.5 |
| 11 | 28 | 94.9 |
| 40 | 40 | 100 |

[a] Determined 4 days after macrophage infection with Y strain trypomastigotes. Inhibition [%] was determined in comparison to untreated infected cells. Data are from one single experiment. Bdz = benznidazole.

## Discussion

There is a need for novel anti-*T. cruzi* drugs. Thiazolidinones are heterocyclic compounds well known for their antiprotozoal activities.[35–38] After screening the activity of 60 thiazolidinic derivatives, we previously identified a potent anti-*T. cruzi* thiazolidinone (18).[24] This compound selectively inhibited the trypanosomal protease cruzain but not its mammalian homologous cathepsin L. Of note, compound 18 achieved inhibitory property against cruzain without exhibiting nonspecific and promiscuous binding properties, a characteristic observed for thiazolidinones of very low molecular weight.[39] Moreover, this compound presented low cytotoxicity towards host cells, no apparent toxicity in mice and reduced blood parasitemia in mice when administrated orally. As a limitation, thiazolidinone 18 was less efficient in reducing acute infection than benznidazole. Therefore, compound 18 was used here as a structural prototype for the synthesis of a series of novel thiazolidinones.

The employed structural planning for the design of compounds 4a–p aimed at causing a disruption in the molecular planarity between the phenoxy group and the thiazolidinic ring. This was achieved by the attachment of an aryl group in the iminic carbon of this class of compounds. As highlighted in Figure 2, this produced derivatives with higher conformational restriction compared with the prototype (18). The pharmacological evaluation of compounds 4a–p confirmed that the disruption of the planarity changed the bioactive profile of this compound class. Importantly, this led to the identification of derivatives with an enhanced antiparasitic activity compared with known thiazolidinones, such as compound 18.

Regarding the antiparasitic activity for trypomastigotes, we found that the attachment of a phenyl ring produced an active thiazolidinone, which was, however, less potent than benznidazole. Replacing the phenyl with a pyridinyl ring was deleterious for antiparasitic activity, suggesting certain structural requirements for placing an aryl ring at the iminic carbon. In fact, the investigation of substituents attached to the phenyl ring revealed interesting SARs. We found substituents that retained (4-Cl, 4-morpholinyl), enhanced (4-Br, 4-phenyl, 4-thiomorpholinyl) or removed (4-CH$_3$, 4-CH$_3$O, 4-F) activity against trypomastigotes in comparison to the nonsubstituted thiazolidinone. Among the substituents that led to an enhanced anti-*T. cruzi* activity, 4-bromo (4h) and biphenyl (4l) were the most promising in terms of potency and selectivity. These compounds were able to inhibit the proliferation of epimastigotes and were toxic for *T. cruzi* but displayed low cytotoxicity towards host cells. Though compounds 4h and 4l both have hydrophobic and bulky substituents, other substituents containing similar properties, such as *tert*-butyl or phenoxy, did not produce active antiparasitic agents. This implies that there are unknown structural requirements involved in 4h and 4l that provide the observed antiparasitic activity.

Moreover, we observed that only 4n (piperidinyl) and 4p (thiomorpholinyl) inhibited cruzain activity whereas other derivatives did not. The literature describes some diastereoisomers with different cruzain inhibitory properties.[40] However, the isomeric ratios for 4n and 4p are not different from the rest of the chemical series. Therefore, the observed inhibitory properties for cruzain are likely due to the substituents present in 4n and 4p. For compounds 4n and 4p, the attachment of a piperidinyl or thiomorpholinyl produced compounds with inhibitory property against cruzain; however, this was abolished when a morpholinyl substituent was attached. In fact, cruzain docking of 4n showed that the piperidinyl group is oriented in a hydrophobic pocket with the participation of π–π T-shaped interactions. The same is not observed for compounds 4b and 4o, which explains their lack of inhibitory activity against cruzain.

Compound 4h was selected as an anti-*T. cruzi* lead compound because it exhibited the highest selectivity among the thiazolidinones studied here. Under 4h treatment, in vitro parasite development and invasion in host cells was substantially reduced. This activity was more pronounced even than that observed with benznidazole-treated parasites. Moreover, the treatment with this compound caused alterations in the Golgi apparatus and the ER morphology of *T. cruzi*, whereas little or no effects were observed in the kinetoplast and cell nucleus morphology. Therefore, this compound exerts its antiparasitic activity by altering organelle morphology, which ultimately destroys parasite cells, similar to the mode of action of a parasiticidal agent. In agreement to this, we observed that 4h caused parasite cell death through a necrotic process.

With regard to the activity in infected mice during the acute phase, 4h reduced the blood parasitemia in a dose-dependent manner and exhibited a potency similarly to that observed in benznidazole-receiving mice. When compared to untreated infected mice, thiazolidinone 4h reduced 97% of blood parasitemia, while at the same dose, the reduction observed for the previously reported thiazolidinone 18 was 89%.[24] Therefore, a potency enhancement of the in vivo antiparasitic activity was achieved from the first-generation thiazolidinone 18 to the new generation described here (4h). Regarding toxicity in mice, 4h was not lethal in doses up to 600 mg kg$^{-1}$, which is several times higher than the dose used to reduce blood parasitemia. Altogether, these results reinforced the notion that thiazolidinone 4h is a selective anti-*T. cruzi* agent. A pharmacokinetic analysis as well as identification of its mechanism of action should be determined in the course of further investigation. However, our preliminary results already show that the combination of thiazolidinone 4h plus benznidazole is additive in reducing in vitro *T. cruzi* infection. This finding indicates that thiazolidinone 4h could be a suitable partner for anti-Chagas drug combinations. This is an important parameter for new anti-Chagas drug candidates, since an effective treatment will likely contain a drug combination to improve the efficacy of the treatment and to reduce the chance of developing parasite resistance.[41]

## Conclusions

Thiazolidinones are a family of well-known antiparasitic compounds. Here, we prepared a series of new thiazolidinones 4a–p, which were designed to be potential anti-*Trypanosoma cruzi* compounds targeting the trypanosomal protease cruzain. In

fact, we found these compounds are antiparasitic agents and have a high degree of selectivity. Our structure–activity relationship (SAR) studies revealed structural determinants for antiparasitic activity and led to the identification of thiazolidinone derivatives, which displayed similar potencies to benznidazole. Specifically, we demonstrated that thiazolidinone **4h** has strong antiparasitic activity, low cytotoxicity toward host cells and achieves its anti-*T. cruzi* activity as a parasiticidal agent. Most thiazolidinones, including active compound **4h**, did not inhibit cruzain activity, but these compounds affected the Golgi apparatus as well as ER morphology and produced atypical cytosolic vacuoles, which ultimately is followed by a necrotic parasite cell death. Consistent with in vitro antiparasitic activity, thiazolidinone **4h** reduced parasitemia in a mice model of acute infection. Importantly, this compound displayed low toxicity in mice and exhibited additive antiparasitic activity when combined with benznidazole.

## Experimental Section

### Chemistry

Synthetic protocols and spectral data for compounds are described in the Supporting Information.

### Docking

The structures of all compounds were obtained by application of the RM1 method,[42] available as part of the SPARTAN 08′ program,[43] using internal default settings for convergence criteria. Some of these new molecules were synthesized as racemic mixtures; therefore, the molecular modeling treated the two isomers (*R* and *S*) independently, when appropriate, and the docking procedure used both isomers for each compound. Docking calculations and analysis were carried using the structure of *T. cruzi* cruzain (PDBID: 3IUT) as the target, which is composed of a co-crystallized complex with inhibitor (referred as "KB2").[13] The active site was defined as all atoms within a radius of 6.0 Å from the co-crystalized ligand. Residues Gln19, Cys25, Ser61, Leu67, Met68, Asn70, Asp161, His162, Trp184 and Glu208 were treated as flexible during the calculations, using a conformation library for each one. The GOLD 5.1 program[44] was used for docking calculations, followed by Binana program,[45] which was used to analyze the molecular interactions present in the best docking solutions, using default setting, except for hydrogen bond distance, which was changed to a maximum of 3.5 Å. Figures were generated with Pymol (version 1.3r1 edu).[46]

### Biology

*Animals*: Female BALB/c mice, aged 6–8 weeks, were supplied by the animal house of Centro de Pesquisas Gonçalo Moniz (Fundação Oswaldo Cruz, Bahia, Brazil) and Centro de Pesquisas Aggeu Magalhaes (Fundação Oswaldo Cruz, Pernambuco, Brazil). Mice were maintained in sterilized cages under a controlled environment, receiving a balanced diet for rodents and water ad libitum. All experiments were carried out in accordance with the recommendations of ethical guidelines and were approved by the local Animal Ethics Committee.

*Cell culture*: Epimastigotes of a Dm28c strain (discrete typing unit I) were maintained at 26 °C in liver infusion tryptose (LIT) medium (Life Technologies, Carlsbad, CA, USA) supplemented with 10% fetal bovine serum (FBS, Life Technologies), 1% hemin (Sigma–Aldrich, St. Louis, MO, USA), 1% R9 medium (Sigma–Aldrich), and 50 µg mL$^{-1}$ gentamycin (Novafarma, Anápolis, GO, Brazil). Metacyclic trypomastigotes of Y strain (discrete typing unit II) were obtained from the supernatant of infected LLC-MK2 cells and maintained in RPMI-1640 medium (Sigma–Aldrich) supplemented with 10% FBS and 50 µg mL$^{-1}$ gentamycin at 37 °C and 5% CO$_2$. Splenocytes were collected from BALB/c mice and cultivated in RPMI-1640 medium supplemented with 10% FBS and 50 µg mL$^{-1}$ gentamycin. Peritoneal exudate macrophages were elicited by intraperitoneal injection of sodium thioglycollate in BALB/c mouse.

*Cytotoxicity in splenocytes*: Splenocytes of BALB/c mice (200 µL) were placed into 96-well plates at $5 \times 10^6$ cells/well. Compounds were added in a serial dilution (1.1, 3.3, 11, 33 and 100 µg mL$^{-1}$) in triplicate. To each well, an aliquot of compound suspended in dimethyl sulfoxide (DMSO) was added. Negative (untreated) and positive (saponin, Sigma–Aldrich) controls were measured in each plate, which was incubated for 24 h at 37 °C and 5% CO$_2$. After incubation, [$^3$H]-thymidine (1.0 µCi mL$^{-1}$, PerkinElmer, Waltham, MA, USA) was added to each well, and the plate was returned to the incubator. Cells were then transferred to a filter paper using a cell harvester and measured using a liquid scintillation counter (WALLAC 1209, Rackbeta Pharmacia, Stockholm, Sweden). [$^3$H]-Thymidine incorporation [%] was measured, and the highest noncytotoxic concentration was determined using triplicates.

*Antiproliferative activity for epimastigotes*: Epimastigotes were counted in a hemocytometer, and 200 µL were dispensed into 96-well plates at 10$^6$ cells/well. Compounds were added in a serial dilution (1.1, 3.3, 11, 33 and 100 µg mL$^{-1}$) in triplicate. The plate was incubated for 5 days at 26 °C, and aliquots of each well were collected for counting the number of viable parasites using a Neubauer chamber. The percentage of inhibition was calculated in relation to untreated cultures. IC$_{50}$ values were calculated using nonlinear regression on Prism 4.0 (GraphPad). Results are from one single experiment.

*Toxicity for trypomastigotes*: Trypomastigotes were collected from the supernatant of LLC-MK2 cells, and 200 µL were aliquoted into 96-well plate in an axenic media at $4 \times 10^5$ cells/well. Compounds were added in a serial dilution (1.1, 3.3, 11, 33 and 100 µg mL$^{-1}$) in triplicate. The plate was incubated for 24 h at 37 °C and 5% of CO$_2$. Aliquots of each well were collected, and the number of viable parasites, based on parasite motility, was counted in a Neubauer chamber. The percentage of inhibition was calculated in relation to untreated cultures. CC$_{50}$ calculation was also carried out using nonlinear regression with Prism 4.0 (GraphPad). Two independent experiments were performed.

*Intracellular parasite development*: Macrophages were seeded at $2 \times 10^5$ cells/well for 24 h in a 24-well plate with rounded coverslips on the bottom in RPMI-1640 medium supplemented with 10% FBS. Macrophages were infected with trypomastigotes at a ratio of 10 parasites per macrophage for 2 h. Unbound trypomastigotes were removed by successive washes with saline. Each compound was dissolved in 5% DMSO and saline in a serial dilution, in triplicate. Compounds remained on the cell culture for 6 h prior to removal and addition of fresh media. The plate was incubated for 4 days at 37 °C and 5% CO$_2$. Cells were fixed in MeOH, stained with Giemsa and manual counting of at least 100 cells per slide was done using an optical microscope (Model CX41, Olympus, Tokyo, Japan). The

percentages of infected macrophages and mean numbers of amastigotes per 100 infected macrophages were determined. To calculate IC$_{50}$ values, the percentage of infected macrophages in comparison to untreated infected macrophages was used.

*Drug combination evaluation*: The combination of thiazolidinone **4h** plus benznidazole was evaluated in the in vitro infection assay (described above). To this end, compounds were tested in the same concentration of their IC$_{50}$ values as well as in higher concentrations.

*Parasite invasion*: Macrophages ($10^5$ cells mL$^{-1}$) were plated onto 13 mm glass coverslips in a 24-well plate and maintained for 24 h. Y strain trypomastigotes were added at $10^7$ cells mL$^{-1}$, followed by addition of compound **4h**. Amphotericin B (Fungizone, Life Technologies) and benznidazole (Lafepe, Recife, PE, Brazil) were used as reference compounds. The plate was incubated for 2 h at 37 °C and 5% CO$_2$. Unbound parasites were then removed by successive washes with saline, and the RPMI medium was replaced. After 2 h of incubation, the number of infected cells was counted by optical microscopy using standard Giemsa staining.

*Inhibition of cruzain activity*: Recombinant cruzain was kindly provided by Dr. Anna Tochowicz and Dr. James H. McKerrow from the University of California, San Francisco (CA, USA). Cruzain activity was measured by monitoring the cleavage of the fluorogenic substrate Z-Phe-Arg-aminomethylcoumarin (Z-FR-AMC, Sigma–Aldrich) using a Synergy 2 microplate reader (Biotek) from the Center of Flow Cytometry and Fluorimetry in the Biochemistry and Immunology Department (UFMG, Brazil) with filters for $\lambda = 340$ nm (excitation) and $\lambda = 440$ nm (emission). All assays were performed in 0.1 M NaOAc (pH 5.5) and in the presence of 5 mM dithiothreitol. The final concentration of cruzain was 0.5 nM, and the substrate concentration was 2.5 μM ($K_m = 1.0$ μM). Assays were conducted in presence of 0.01% Triton X-100. Compounds were screened at 100 μM, after pre-incubation for 10 min with the enzyme prior to the addition of Z-FR-AMC. In all assays, fluorescence was monitored for 5 min after addition of the substrate and activity was calculated in relation to DMSO control. If the cruzain inhibition was higher than 70% at 100 μM, IC$_{50}$ values were determined by using at least seven inhibitor concentrations. Each compound concentration was tested in triplicate and data were analyzed with Prism 5.0 (GraphPad).

*Electron microscopy analysis*: Trypomastigotes ($3 \times 10^7$ cells mL$^{-1}$) were treated with **4h** (4.0 μM) for 24 h. Parasites were fixed in 2% formaldehyde and 2.5% glutaraldehyde (Electron Microscopy Sciences, Philadelphia, PA, USA) in sodium cacodylate buffer (0.1 M, pH 7.2) for 1 h at RT, washed 3× with sodium cacodylate buffer (0.1 M, pH 7.2), and post-fixed with a 1% solution of osmium tetroxide (Sigma–Aldrich) for 1 h. After dehydration with acetone, trypomastigotes were embedded in Poly/Bed (PolyScience, Dallas, TX, USA), sectioned, stained with uranyl acetate and lead citrate and analyzed using a JEOL TEM-1230 transmission electron microscope (Acworth, GA, USA). Mouse macrophages were infected with Y strain trypomastigotes. Cell cultures were washed with saline to remove unbound parasites, followed by the addition of **4h** (5.0 μM) and incubation for 6 h at RT. Cell cultures were processed as described above for collecting TEM images.

*Flow cytometry analysis*: Trypomastigotes ($10^7$ cells mL$^{-1}$) were treated with **4h** (4.0, 8.0 and 12 μM) and incubated for 72 h at 37 °C. Aliquots were collected in the intervals of 24–72 h and incubated for 45 min with propidium iodide (PI) and annexin V using the annexin V–FITC apoptosis detection kit (BioLegend, San Diego, CA, USA) according to the manufacturer instructions. Data acquisition and analyses were performed using FACS Calibur flow cytometer (Becton Dickinson, San Jose, CA, USA) and FlowJo software (Tree Star, Ashland, OR, USA), respectively. A total of 20 000 events were acquired. Two independent experiments were performed.

*Acute toxicity in mice*: Uninfected BALB/c mice (female, 7–9 weeks old) were randomly divided in groups ($n = 3$). Oral administration of **4h** was given by gavage in one single dose of 150, 300 or 600 mg kg$^{-1}$ in 20% DMSO/saline as vehicle. After treatment, survival was monitored for 14 days. The same experiment was repeated using $n = 6$ per group. Heparinized blood samples were collected 24 h after treatment for biochemical analysis of serum components. Readings were performed in an Analyst platform (Hemagen Diagnostics, Colombia, MD, USA) for 16 biochemical components. Biochemical readings were compared to negative control (received vehicle only).

*Infection in mice*: BALB/c mice (female, 6–8 weeks old) were infected with bloodstream trypomastigotes (Y strain) by intraperitoneal injection of $10^4$ parasites in 100 μL of saline solution. Mice were randomly divided in groups ($n = 6$ per group). After day 5 of post-infection, treatment with **4h** was given orally by gavage once a day for five consecutive days. For the positive control group, benznidazole was given orally. As recommended by standard protocols, infection was monitored daily by counting the number of motile parasites in 5 μL of fresh blood sample drawn from the lateral tail vein.[47] Mortality was recorded daily until day 30 after the end of treatment.

*Statistical analysis*: To determine the statistical significance of each group in the in vitro and in vivo experiments, the one-way ANOVA test and the Bonferroni for multiple comparisons were used. A $p$ value $< 0.05$ was considered significant.

### Supporting Information

Please see the Supporting Information for synthetic protocols, spectral data for compounds and a table with toxicological results. CCDC 936127 contains the supplementary crystallographic data (**4q**) of this paper. These data can be obtained free of charge from The Cambridge Crystallographic Data Centre (Cambridge, UK) via www.ccdc.cam.ac.uk).

### Acknowledgements

[1] J. A. Urbina, *Clin. Infect. Dis.* **2009**, *49*, 1685–1687.

[2] M. P. Barrett, R. J. Burchmore, A. Stich, J. O. Lazzari, A. C. Frasch, J. J. Cazzulo, S. Krishna, *Lancet* **2003**, *362*, 1469–1480.

[3] A. Rassi, A. Rassi, Jr., J. A. Marin-Neto, *Lancet* **2010**, *375*, 1388–1402.

[4] F. S. Machado, L. A. Jelicks, L. V. Kirchhoff, J. Shirani, F. Nagajyothi, S. Mukherjee, R. Nelson, C. M. Coyle, D. C. Spray, A. C. de Carvalho, F. Guan, C. M. Prado, M. P. Lisanti, L. M. Weiss, S. P. Montgomery, H. B. Tanowitz, *Cardiol. Rev.* **2012**, *20*, 53–65.

[5] S. Gupta, X. Wan, M. P. Zago, V. C. Sellers, T. S. Silva, D. Assiah, M. Dhiman, S. Nuñez, J. R. Petersen, J. C. Vázquez-Chagoyán, J. G. Estrada-Franco, N. J. Garg, *PLoS Neglected Trop. Dis.* **2013**, *7*, e2018.

[6] M. B. P. Soares, R. S. Lima, B. S. F. Souza, J. F. Vasconcelos, L. L. Rocha, R. R. Dos Santos, S. Iacobas, R. C. Goldenberg, M. P. Lisanti, D. A. Iacobas, H. B. Tanowitz, D. C. Spray, A. C. Campos de Carvalho, *Cell Cycle* **2011**, *10*, 1448–1455.

[7] S. G. Macambira, J. F. Vasconcelos, C. R. Costa, W. Klein, R. S. Lima, P. Guimarães, D. T. Vidal, L. C. Mendez, R. Ribeiro-Dos-Santos, M. B. P. Soares, *FASEB J.* **2009**, *23*, 3843–3850.

[8] R. A. Cutrullis, T. J. Poklépovich, M. Postan, H. L. Freilij, P. B. Petray, *Int. Immunopharmacol.* **2011**, *11*, 1024–1031.

[9] J. M. Kraus, H. B. Tatipaka, A. S. McGuffin, N. K. Chennamaneni, M. Karimi, J. Arif, C. L. Verlinde, F. S. Buckner, M. H. Gelb, *J. Med. Chem.* **2010**, *53*, 3887–3898.

[10] A. Gerpe, G. Alvarez, D. Benítez, L. Boiani, M. Quiroga, P. Hernández, M. Sortino, S. Zacchino, M. González, H. Cerecetto, *Bioorg. Med. Chem.* **2009**, *17*, 7500–7509.

[11] S. P. Fricker, R. M. Mosi, B. R. Cameron, I. Baird, Y. Zhu, V. Anastassov, J. Cox, P. S. Doyle, E. Hansell, G. Lau, J. Langille, M. Olsen, L. Qin, R. Skerlj, R. S. Wong, Z. Santucci, J. H. McKerrow, *J. Inorg. Biochem.* **2008**, *102*, 1839–1845.

[12] M. E. Caputto, A. Ciccarelli, F. Frank, A. G. Moglioni, G. Y. Moltrasio, D. Vega, E. Lombardo, L. M. Finkielsztein, *Eur. J. Med. Chem.* **2012**, *55*, 155–163.

[13] K. Brak, I. D. Kerr, K. T. Barrett, N. Fuchi, M. Debnath, K. Ang, J. C. Engel, J. H. McKerrow, P. S. Doyle, L. S. Brinen, J. A. Ellman, *J. Med. Chem.* **2010**, *53*, 1763–1773.

[14] P. S. Doyle, C. K. Chen, J. B. Johnston, S. D. Hopkins, S. S. Leung, M. P. Jacobson, J. C. Engel, J. H. McKerrow, L. M. Podust, *Antimicrob. Agents Chemother.* **2010**, *54*, 2480–2488.

[15] F. S. Buckner, M. T. Bahia, P. K. Suryadevara, K. L. White, D. M. Shackleford, N. K. Chennamaneni, M. A. Hulverson, J. U. Laydbak, E. Chatelain, I. Scandale, C. L. Verlinde, S. A. Charman, G. I. Lepesheva, M. H. Gelb, *Antimicrob. Agents Chemother.* **2012**, *56*, 4914–4921.

[16] F. Villalta, M. C. Dobish, P. N. Nde, Y. Y. Kleshchenko, T. Y. Hargrove, C. A. Johnson, M. R. Waterman, J. N. Johnston, G. I. Lepesheva, *J. Infect. Dis.* **2013**, *208*, 504–511.

[17] X. Du, C. Guo, E. Hansell, P. S. Doyle, C. R. Caffrey, T. P. Holler, J. H. McKerrow, F. E. Cohen, *J. Med. Chem.* **2002**, *45*, 2695–2707.

[18] D. C. Greenbaum, Z. Mackey, E. Hansell, P. Doyle, J. Gut, C. R. Caffrey, J. Lehrman, P. J. Rosenthal, J. H. McKerrow, K. Chibale, *J. Med. Chem.* **2004**, *47*, 3212–3219.

[19] A. C. L. Leite, R. S. de Lima, D. R. M. Moreira, M. V. O. Cardoso, A. C. G. Brito, L. M. F. Santos, M. Z. Hernandes, A. C. Kiperstok, R. S. de Lima, M. B. P. Soares, *Bioorg. Med. Chem.* **2006**, *14*, 3749–3457.

[20] J. M. dos Santos Filho, A. C. L. Leite, B. G. de Oliveira, D. R. M. Moreira, M. S. Lima, M. B. P. Soares, L. F. C. C. Leite, *Bioorg. Med. Chem.* **2009**, *17*, 6682–6891.

[21] J. M. dos Santos Filho, D. R. M. Moreira, C. A. de Simone, R. S. Ferreira, J. H. McKerrow, C. S. Meira, E. T. Guimarães, M. B. P. Soares, *Bioorg. Med. Chem.* **2012**, *20*, 6423–6433.

[22] A. C. L. Leite, D. R. M. Moreira, M. V. O. Cardoso, M. Z. Hernandes, V. R. A. Pereira, R. O. Silva, A. C. Kiperstok, M. S. Lima, M. B. P. Soares, *ChemMedChem* **2007**, *2*, 1339–1345.

[23] M. Z. Hernandes, M. M. Rabello, A. C. L. Leite, M. V. O. Cardoso, D. R. M. Moreira, D. J. Brondani, C. A. Simone, L. C. Reis, M. A. Souza, V. R. A. Pereira, R. S. Ferreira, J. H. McKerrow, *Bioorg. Med. Chem.* **2010**, *18*, 7826–7835.

[24] D. R. M. Moreira, S. P. Costa, M. Z. Hernandes, M. M. Rabello, G. B. O. Filho, C. M. de Melo, L. F. da Rocha, C. A. de Simone, R. S. Ferreira, J. R. Fradico, C. S. Meira, E. T. Guimarães, R. M. Srivastava, V. R. A. Pereira, M. B. P. Soares, A. C. L. Leite, *J. Med. Chem.* **2012**, *55*, 10918–10936.

[25] C. L. Donnici, M. H. Araújo, H. S. Oliveira, D. R. M. Moreira, V. R. A. Pereira, M. A. Souza, M. C. Castro, A. C. L. Leite, *Bioorg. Med. Chem.* **2009**, *17*, 5038–5043.

[26] M. Ishikawa, Y. Hashimoto, *J. Med. Chem.* **2011**, *54*, 1539–1554.

[27] E. J. Barreiro, A. E. Kümmerle, C. A. M. Fraga, *Chem. Rev.* **2011**, *111*, 5215–5246.

[28] Ö. Ö. Güven, *ARKIVOC* **2007**, 142–147.

[29] G. M. Allan, N. Vicker, H. R. Lawrence, H. J. Tutill, J. M. Day, M. Huchet, E. Ferrandis, M. J. Reed, A. Purohit, B. V. Potter, *Bioorg. Med. Chem.* **2008**, *16*, 4438–4456.

[30] P. Vicini, A. Geronikaki, K. Anastasia, M. Incerti, F. Zani, *Bioorg. Med. Chem.* **2006**, *14*, 3859–3864.

[31] M. H. Bolli, S. Abele, C. Binkert, R. Bravo, S. Buchmann, D. Bur, J. Gatfield, P. Hess, C. Kohl, C. Mangold, B. Mathys, K. Menyhart, C. Müller, O. Nayler, M. Scherz, G. Schmidt, V. Sippel, B. Steiner, D. Strasser, A. Treiber, T. Weller, *J. Med. Chem.* **2010**, *53*, 4198–4211.

[32] A. P. Liesen, T. M. de Aquino, C. S. Carvalho, V. T. Lima, J. M. de Araújo, J. G. de Lima, A. R. de Faria, E. J. de Melo, A. J. Alves, E. W. Alves, A. Q. Alves, A. J. S. Góes, *Eur. J. Med. Chem.* **2010**, *45*, 3685–3691.

[33] R. S. Ferreira, C. Bryant, K. K. Ang, J. H. McKerrow, B. K. Shoichet, A. R. Renslo, *J. Med. Chem.* **2009**, *52*, 5005–5058.

[34] M. A. Vannier-Santos, S. L. De Castro, *Curr. Drug Targets* **2009**, *10*, 246–260.

[35] C. Pizzo, C. Saiz, A. Talevi, L. Gavernet, P. Palestro, C. Bellera, L. B. Blanch, D. Benítez, J. J. Cazzulo, A. Chidichimo, P. Wipf, S. G. Mahler, *Chem. Biol. Drug Des.* **2011**, *77*, 166–177.

[36] H. E. Cummings, J. Barbi, P. Reville, S. Oghumu, N. Zorko, A. Sarkar, T. L. Keiser, B. Lu, T. Rückle, S. Varikuti, C. Lezama-Davila, M. D. Wewers, C. Whitacre, D. Radzioch, C. Rommel, S. Seveau, A. R. Satoskar, *Proc. Natl. Acad. Sci. USA* **2012**, *109*, 1251–1256.

[37] N. Zelisko, D. Atamanyuk, O. Vasylenko, P. Grellier, R. Lesyk, *Bioorg. Med. Chem. Lett.* **2012**, *22*, 7071–7074.

[38] T. L. de B. Moreira, A. F. S. Barbosa, P. Veiga-Santos, C. Henriques, A. Henriques-Pons, S. L. Galdino, M. C. de Lima, I. R. Pitta, W. de Souza, T. M. de Carvalho, *Int. J. Antimicrob. Agents* **2013**, *41*, 183–187.

[39] T. Mendgen, C. Steuer, C. D. Klein, *J. Med. Chem.* **2012**, *55*, 743–753.

[40] N. C. Romeiro, G. Aguirre, P. Hernández, M. González, H. Cerecetto, I. Aldana, S. Pérez-Silanes, A. Monge, E. J. Barreiro, L. M. Lima, *Bioorg. Med. Chem.* **2009**, *17*, 641–652.

[41] S. Cencig, N. Coltel, C. Truyens, Y. Carlier, *Int. J. Antimicrob. Agents* **2012**, *40*, 527–532.

[42] G. B. Rocha, R. O. Freire, A. M. Simas, J. J. Stewart, *J. Comput. Chem.* **2006**, *27*, 1101–1111.

[43] Spartan '08 Tutorial and User's Guide; Wavefunction: Irvine, CA, **2008**: http://www.wavefun.com/products/spartan.html (accessed: August 2013).

[44] Gold software, version 5.1, Cambridge Crystallographic Data Centre: http://www.ccdc.cam.ac.uk (accessed: August 2013).

[45] J. D. Durrant, J. A. Mccammon, *J. Mol. Graphics Modell.* **2011**, *29*, 888–893.

[46] W. L. DeLano. The PyMOL Molecular Graphics System, DeLano Scientific, San Carlos, CA, **2002**: http://www.pymol.org (accessed: August 2013).

[47] A. J. Romanha, S. L. Castro, M. N. Soeiro, J. Lannes-Vieira, I. Ribeiro, A. Talvani, B. Bourdin, B. Blum, B. Olivieri, C. Zani, C. Spadafora, E. Chiari, E. Chatelain, G. Chaves, J. E. Calzada, J. M. Bustamante, L. H. Freitas-Junior, L. I. Romero, M. T. Bahia, M. Lotrowska, M. B. Soares, S. G. Andrade, T. Armstrong, W. Degrave, Z. A. Andrade, *Mem. Inst. Oswaldo Cruz* **2010**, *105*, 233–238.